

**CORRELATION OF OBSERVED BUILDING PERFORMANCE
WITH MEASURED GROUND MOTION**

Stephanie A. King
Hart-Weidlinger, Weidlinger Associates, Inc.

Anne S. Kiremidjian, Pooya Sarabandi, and Dimitris Pachakis
John Blume Earthquake Engineering Center, Stanford University

Abstract

This paper describes results of the CSMIP-funded project to develop correlations of observed building performance with measured ground motion. Much of the information presented in the paper is taken from King et al. (2002), which described the progress of the project to date at last year's SMIP02 Seminar. Motion-damage relationships in the form of lognormal fragility curves and damage probability matrices have been developed for wood frame, steel moment frame, and concrete frame buildings – building types for which there are enough samples in the database to warrant statistical analysis. The ground motion parameters that were found to exhibit relatively higher correlations with building performance were used in the analysis. Building performance is characterized in terms of damage states and performance levels. The resulting relationships are compared to those published in ATC-13 (ATC, 1985) and HAZUS99 (FEMA, 1999). The comparison shows that the relationships developed in the project are quite different from the published models; however, the loss estimates resulting from the application of the models are similar.

Introduction

Relationships between building performance and ground motion form the core of earthquake loss estimation methodologies, and are also used for structural analysis studies and in the design code formulation process. Currently-used motion-damage relationships are based primarily on models developed from expert opinion, such as ATC-13 (ATC, 1985), or models that combine analytical model results with expert opinion, such as HAZUS99 (FEMA, 1999). Attempts have been made to update the published motion-damage relationships with empirical data collected after damaging earthquakes (see Anagnos et al., 1995). Small improvements have been made to models for specific building types, but typically with the use of proprietary insurance loss data with inferred ground motion information.

Following the 1994 Northridge earthquake, an effort was made to systematically document the effects of earthquake shaking on structures adjacent to locations of strong ground motion recordings. The ATC-38 project (ATC, 2000) involved the inspection of more than 500 buildings located near (within 1000 feet of) 30 strong motion recording stations. The resulting database of building characteristic and performance documentation, photos, and strong motion recordings provides a wealth of information for developing new motion-damage relationships

based on non-proprietary empirical data. A similar dataset was also developed following the 1999 Chi-Chi, Taiwan earthquake.

The purpose of the CSMIP-funded project discussed in this paper is to develop motion-damage relationships based on the correlation of observed building performance with measured ground motion parameters. The project tasks include: identifying and collecting appropriate datasets; analyzing, interpreting, and archiving data records; developing motion-damage relationships in the form of damage probability matrices and fragility curves; and illustrating the use of the final relationships. The remainder of this paper discusses these tasks in more detail and presents some key results of the project.

Dataset Collection

In order to develop meaningful and useful motion-damage relationship that correlate building performance to recorded ground motion data, the datasets have to satisfy certain criteria, including:

- Proximity to free-field ground motion recordings – building should be located close enough to strong motion recordings so that the shaking at the building site can be approximated as the shaking at the instrument site. Also, the building should not have any site-specific geologic conditions that might alter the ground shaking at the site.
- Non-proprietary – the datasets should contain information that is available to the general public so that other researchers may use the raw data, with their own proprietary data or with information collected after future earthquakes.
- Sufficient number of data points – statistical relationships will only be meaningful for those building classes with a large enough sample size.
- Consistent building survey information – building performance data should have been collected in a standard format with consistent inspector interpretation of qualitative and quantitative measures of damage.
- Unbiased with respect to building damage – datasets often include information only for damaged buildings. Statistical relationships will not be meaningful unless the datasets include information for both damaged and undamaged buildings.

The first task of the project was to identify and collect datasets that meet the above criteria, which were found to be very stringent. The following datasets were collected for use in the project:

- ATC-38 – Database on the Performance of Structures Near Strong-Motion Recordings: 1994 Northridge, California Earthquake (ATC, 2000)
- LADiv88 – Rutherford and Chekene Database on the Performance of Rehabilitated Unreinforced Masonry Buildings (Retrofitted According to Los Angeles Division 88 Standards) in the 1994 Northridge, California Earthquake (Lizundia and Holmes, 1997)
- SAC – Database on the Performance of Steel Moment Frame Buildings in the 1994 Northridge, California Earthquake (FEMA, 2000)

- Chi-Chi – Degenkolb Database on the Performance of Buildings Near Strong-Motion Recording Stations (Heintz and Poland, 2001)

Following the collection of the building performance datasets, the accompanying strong ground motion data were identified and collected. For the ATC-38 and Chi-Chi building datasets, the strong ground motion data are included as database tables linked via the attribute containing the building identification number. All buildings in these two datasets could be used in the analysis as they are all located very close (within 1000 feet) of the recording stations.

For the SAC and LADiv88 building datasets, only those buildings located near to free-field strong motion recording stations (and on similar site conditions) were extracted from the complete databases. This was done by mapping the building locations in a GIS and overlaying a map of the ground motion recording stations. Two classes of buildings were extracted from their respective datasets – those within 1000 feet of a recording station and those within 1 km of a recording station. The 1000 foot criterion was the approximate distance used in the ATC-38 and Chi-Chi datasets. The 1 km criterion was added so that a sensitivity study of the distance criterion could be done.

The strong ground motion data for the stations identified within the vicinity of the SAC and LADiv88 buildings were obtained from several sources including:

- COSMOS – Consortium of Organizations for Strong-Motion Observation Systems Virtual Data Center, which contains links to strong ground motion from the California Division of Mines and Geology, the U.S. Geological Survey, the U.S. Bureau of Reclamation, and the U.S. Army Corps of Engineers (www.cosmos-eq.org)
- PEER – Pacific Earthquake Engineering Research Center Strong Motion Database (peer.berkeley.edu/smcat/)
- NGDC – National Geophysical Data Center Earthquake Strong Motion CD-ROM (www.ngdc.noaa.gov)

Table 1 shows a general distribution of the buildings extracted from the datasets for use in the project.

Ground Motion Analysis

Several ground motion parameters were identified as potential candidates for correlation with building performance data. The parameters include those deemed relevant to the intended use of the resulting motion-damage relationships, i.e., they are typically computed in loss estimation and design procedures.

The following parameters have been computed and archived for each strong motion data record:

- Time history data parameters (maximum of two horizontal components, average of two horizontal components, and vertical):
 - Peak ground acceleration (*PGA*)

- Peak ground velocity (*PGV*)
- Peak ground displacement (*PGD*)
- ShakeMap Instrumental Intensity (*I_{mm}*)
 From Wald et al. (1999), computed as a function of *PGA* in cm/sec² and *PGV* in cm/sec according to the following:

$$I_{mm} = 3.66 \log(PGA) - 1.66 \quad \text{for } I_{mm} < 7 \quad (1a)$$

$$I_{mm} = 3.47 \log(PGV) + 2.35 \quad \text{for } I_{mm} \geq 7 \quad (1b)$$

- Duration (*T_d*)
 For the total record
 For the time period bracketed by 90% of the cumulative energy
 For the time period bracketed by a 0.05g cut-off acceleration level
- Root mean square acceleration (*a_{RMS}*)
 Computed from the acceleration time history *a(t)* for the three time durations (*T_d*) listed above as follows:

$$a_{RMS} = \sqrt{\frac{1}{T_d} \int_0^{T_d} a(t)^2 dt} \quad (2)$$

- Arias Intensity (*A_I*)
 Computed from the acceleration time history *a(t)* for the three time durations (*T_d*) as follows:

$$A_I = \int_0^{T_d} a(t)^2 dt \quad (3)$$

- Response spectra data parameters (maximum of two horizontal components, average of two horizontal components, and vertical):
 - Acceleration spectrum intensity (*ASI*)
 Computed as the area under the acceleration response spectrum between 0.1 and 0.5 seconds (Von Thum et al., 1988)
 - Effective peak acceleration (*EPA*)
 Computed as the average of the acceleration response spectrum between 0.1 and 0.5 seconds, divided by 2.5 (ATC, 1978)
 - Effective peak velocity (*EPV*)
 Computed as the average of the velocity response spectrum between 0.8 and 1.2 seconds, divided by 2.5 (ATC, 1978)
 - Housner intensity (*S_I*)
 Computed as the area under the pseudo velocity response spectrum between 0.1 and 2.5 seconds (Housner, 1952)
 - Spectral acceleration at several periods (*S_a(T)*)
 - Spectral velocity at several periods (*S_v(T)*)
 - Spectral displacement at several periods (*S_d(T)*)

- Others (not computed, but acquired through map overlays in GIS software):
 - Modified Mercalli Intensity (*MMI*)
 - Site class at the recording station site using the 1997 NEHRP Classification (FEMA, 1997)

Table 1 Approximate Distribution of Building Data for Use in Model Development

Building Type	Number of Building Records	
	Within 1000 ft of station	1000 ft - 1 km from station
Wood Frame	270	
Steel Frame	102	57
Concrete Frame	104	
Concrete Shear Wall	73	
Reinforced Masonry	89	
Unreinforced Masonry (URM)	18	
Rehabilitated URM	54	116
Precast	10	
TOTAL	720	173

Building Response Analysis

The building response datasets were initially analyzed for two purposes – to group the buildings into similar structural classes and to interpret the damage survey information. The grouping of buildings by structural class was done according to the FEMA 310 (FEMA, 1998) model building types shown in Table 2. This classification is similar to that used in the ATC-38 database; however, an important difference is the inclusion of model building type W1A to account for multi-story, multi-unit residences with tuck-under parking. For several of the classes shown in Table 2, the number of data points (see Table 1) was not sufficient to develop motion-damage relationships for those classes. As discussed in the next section, relationships were developed for wood frame, steel moment frame, concrete frame, and concrete shear wall buildings.

The building performance information required standardization in terms of damage to structural and nonstructural components. The following classifications are used for structural and nonstructural (if available) damage or performance:

- ATC-13 (ATC, 1985) – Damage states are as follows:
 - 1 = None = 0% loss
 - 2 = Slight = 0-1% loss
 - 3 = Light = 1-10% loss
 - 4 = Moderate = 10-30% loss
 - 5 = Heavy = 30-60% loss
 - 6 = Major = 60-100% loss
 - 7 = Destroyed = 100% loss

- HAZUS99 (FEMA, 1999) – Damage states are as follows:
 - None = 0% loss
 - Slight = 2% loss
 - Moderate = 10% loss
 - Extensive = 50% loss
 - Complete = 100% loss
- Vision 2000 (SEAOC, 1995) – Performance levels are as follows:
 - Fully Operational = 9-10 = Negligible damage
 - Operational = 7-8 = Light damage
 - Life Safe = 5-6 = Moderate damage
 - Near Collapse = 3-4 = Severe damage
 - Collapse = 1-2 = Complete damage
- FEMA 273/274 (FEMA, 1997) – Performance levels are as follows:
 - Operational = Very light damage
 - Immediate Occupancy = Light damage
 - Life Safety = Moderate damage
 - Collapse Prevention = Severe damage

In addition to the standardization of the structural classes and performance descriptions, the design code year and fundamental period were added to the database attributes associated with each building. The design code year is used to compute the design base shear (in terms of the seismic coefficient) and roof drift limit for each building. The fundamental period is used to compute the demand spectral values as described later in this section. For the general building types, the fundamental period is computed as a function of building height, H , as follows:

Wood frame building, based on Camelo et al. (2001):

$$T = 0.032H^{0.55} \tag{4}$$

Steel frame buildings, based on Chopra et al. (1998):

$$T = 0.035H^{0.80} \tag{5}$$

Reinforced concrete frame buildings, based on Chopra et al. (1998):

$$T = 0.018H^{0.90} \tag{6}$$

Rehabilitated unreinforced masonry buildings, based on UBC 1997 (ICBO, 1997):

$$T = 0.020H^{0.75} \tag{7}$$

Concrete shear wall buildings, based on UBC 1997 (ICBO, 1997):

$$T = 0.020H^{0.75} \tag{8}$$

The seismic demands on the building, in terms of displacement and base shear, have also been computed for each building in the dataset. This allowed for development and evaluation of relationships relating earthquake performance, not only to the recorded and computed ground motion parameters listed in the previous section, but also to seismic demand levels.

Table 2 Model Building Types (from FEMA, 1998)

W1: Wood Light Frames	
W1	Single or multiple family dwellings
W1A	Multi-story, multi-unit residences with open front garages at the first story
W2: Wood Frames, Commercial and Industrial	
S1: Steel Moment Frames	
S1	Stiff diaphragms
S1A	Flexible diaphragms
S2: Steel Braced Frames	
S2	Stiff diaphragms
S2A	Flexible diaphragms
S3: Steel Light Frames	
S4: Steel Frame with Concrete Shear Walls	
S5: Steel Frame with Infill Masonry Shear Walls	
S5	Stiff diaphragms
S5A	Flexible diaphragms
C1: Concrete Moment Frames	
C2: Concrete Shear Wall Buildings	
C2	Stiff diaphragms
C2A	Flexible diaphragms
C3: Concrete Frame with Infill Masonry Shear Walls	
C3	Stiff diaphragms
C3A	Flexible diaphragms
PC1: Precast/Tiltup Concrete Shear Walls	
PC1	Stiff diaphragms
PC1A	Flexible diaphragms
PC2: Precast Concrete Frame	
PC2	Stiff diaphragms
PC2A	Flexible diaphragms
RM1: Reinforced Masonry Bearing Wall with Flexible Diaphragms	
RM2: Reinforced Masonry Bearing Wall with Stiff Diaphragms	
URM: Unreinforced Masonry Bearing Wall	
URM	Stiff diaphragms
URMA	Flexible diaphragms

The estimate of building displacement demand during the recorded earthquake ground motion is computed as the spectral displacement demand normalized by the height of the building to obtain a *spectral drift ratio*. The spectral drift ratio, δ_{S_d} , is calculated by the following:

$$\delta_{S_d} = S_d(T)/H \quad (9)$$

where $S_d(T)$ is the building spectral displacement demand obtained from the 5% damped response spectrum of the earthquake ground motion recorded at or near the building site, and H is the building height.

A minor inconsistency occurs when calculating the spectral drift ratio by Equation 9, due to the fact that the spectral displacement demand, based on an equivalent single degree-of-freedom system (SDOF), is normalized by the building height instead of an equivalent height of the SDOF system. In order to achieve consistency and also so that the demands can be compared to building code drift limits and FEMA 273 drift ratios related to building performance, the spectral drift ratio calculated in Equation 9 can be translated to an estimate of the building *roof drift ratio*. The roof drift ratio, δ_R , is calculated by the following:

$$\delta_R = \delta_{S_d} C_0 = \frac{S_d(T)C_0}{H} \quad (10)$$

where C_0 is a modification factor that translates the spectral displacement demand, which represents the displacement of an equivalent SDOF system, to the roof displacement of the building. The value of C_0 depends on the dynamic characteristics of the building, and is based on the values provided by FEMA 273.

As an improvement to the roof drift ratio computation discussed above, Miranda and Reyes (2002) have suggested the use of alternate modification factors for considering the contribution of additional modes and inelastic behavior in MDOF systems. These modification factors consider the effects of displacement ductility of the structure, the fundamental period of the structure, the number of stories, the lateral load pattern, the stiffness reduction along the height of the structure, and the flexural and shear behavior of the structure. Maximum interstory drift ratio, IDR_{max} , is written as:

$$IDR_{max} = \beta_1 \beta_2 \beta_3 \beta_4 \frac{S_d}{H} \quad (11)$$

where β_1 is a dimensionless factor for the continuous model, assuming a uniform mass distribution, β_2 is the ratio between the maximum interstory drift ratio and the roof drift ratio, β_3 is the ratio of maximum inelastic displacement u_i to the maximum elastic displacement u_e , β_4 is a dimensionless factor that captures the effect of ductility and number of stories of the buildings, H is the height of building in units corresponding to S_d , and S_d is the spectral displacement, evaluated at the predominant period of the structure and a damping ratio of 5%.

The reader is referred to Miranda (1999) and Miranda and Reyes (2002) for the equations to compute the modification factors ($\beta_1, \beta_2, \beta_3, \beta_4$) given in Equation 11.

Model Development

The model development first focused on the identification of strong correlations between building performance and measured ground motion parameters. Empirical damage probability matrices were developed for all building performance descriptors and the corresponding ground motion or building demand parameters. Damage probability matrices (DPMs) show the conditional probability of being in a discrete damage state or performance level as a function of

the input ground motion or building demand level, which can be a discrete value (e.g., MMI) or a range of values (e.g., PGA). For the areas of strong correlation, fragility curves were developed in the form of lognormal probability distributions following the method outlined in Singhal and Kiremidjian (1996). Fragility curves show the conditional probability of being equal to or exceeding a given damage state or performance level as a function of the ground motion or building demand parameter. Final DPMs were derived from the fragility functions by discretizing the continuous distributions. Figure 1 illustrates the relationship between DPMs, probability distributions, and fragility curves.

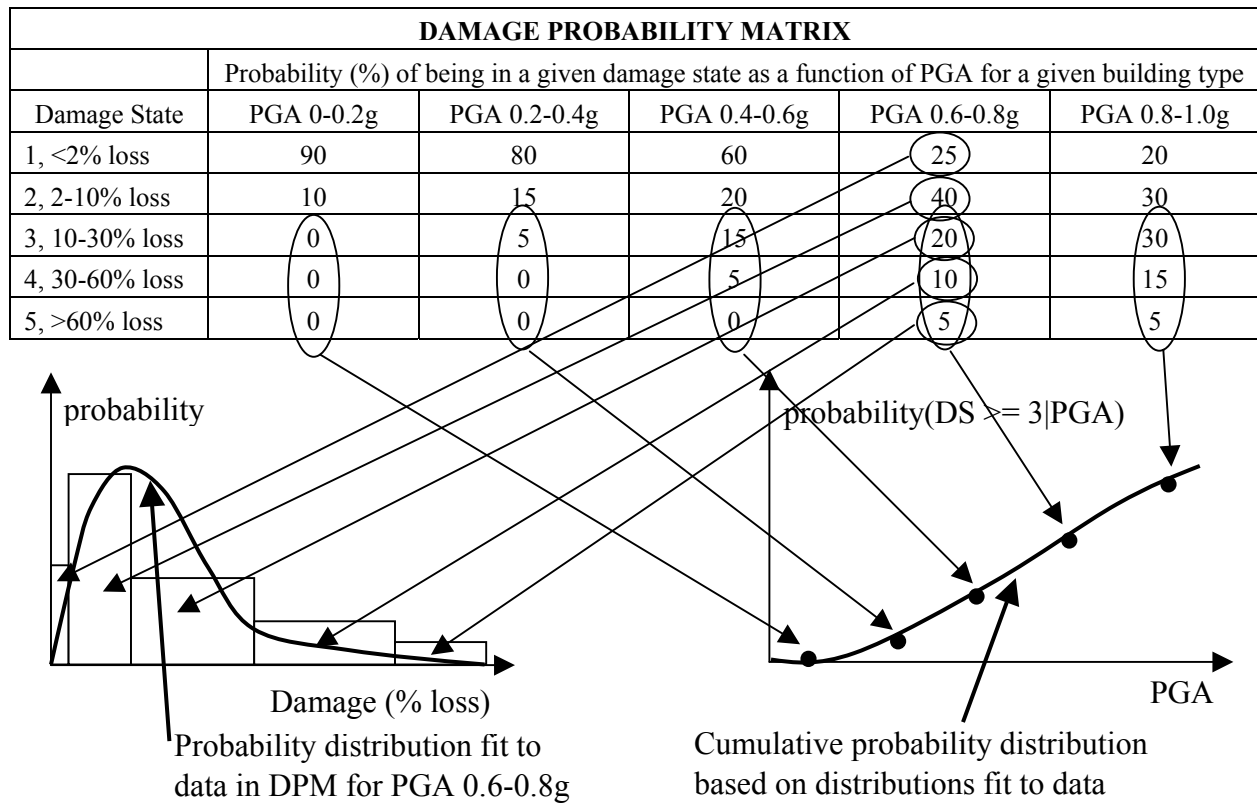


Figure 1 Illustration of DPM, probability distribution fit, and fragility curve.

Sample Results

Motion-damage relationships were developed for wood frame, steel frame, and concrete frame buildings using data from the 1994 Northridge earthquake and the 1999 Chi-Chi, Taiwan earthquake. Due to space limitations for the paper, only wood frame (class W1) building results will be summarized here. The final project report discusses the results for the other building types and also includes an appendix with a complete set of the motion-damage relationships developed in the project, including lognormal fragility parameters and curves.

Fragility functions were developed for the wood frame building class for the following ground motion measures that exhibited relatively higher correlation with building performance: spectral displacement (S_d), Modified Mercalli Intensity (MMI), Instrumental Intensity (I_{MM}),

effective peak velocity (EPV), maximum interstory drift ratio (IDR_{max}), spectral drift ratio (δ_R), peak ground velocity (PGV), spectral velocity (S_v), root mean square acceleration (RMS), Housner Intensity (HI), peak ground displacement (PGD), spectral acceleration (S_a), peak ground acceleration (PGA), and bracketed duration (T_b). Figures 2 and 3 show sample lognormal fragility curves for wood frame buildings. Figure 2 shows the probability of being in or exceeding the ATC-13 damage states as a function of peak ground acceleration, and Figure 3 shows the probability of being in or exceeding the FEMA 273 performance levels as a function of peak ground displacement.

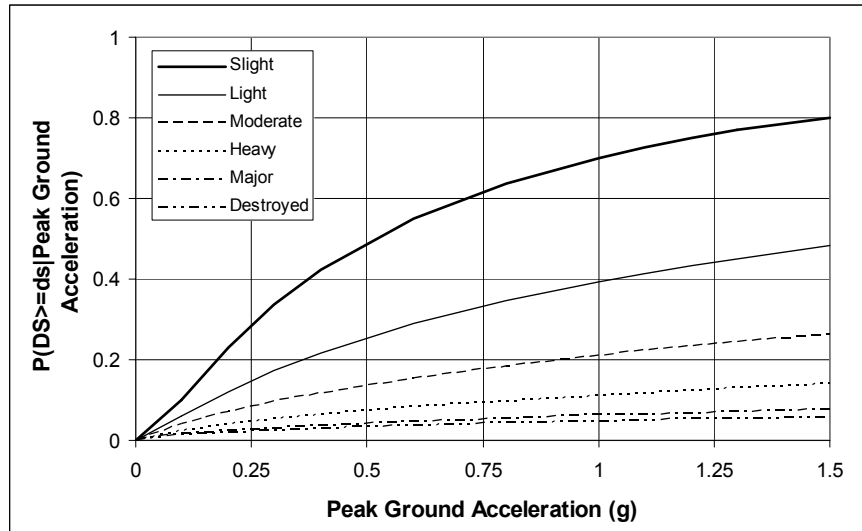


Figure 2 Lognormal fragility curves for W1 buildings and ATC-13 damage states, conditional on peak ground acceleration.

Figure 4 shows a comparison of the lognormal fragility curves conditional on spectral displacement for wood frame buildings published in HAZUS99 (moderate code W1) and as computed in this project. It can be seen in Figure 4 that for the estimated fragility curves, the differences between the various damage states are small, while the HAZUS99 curves for the various damage states are quite distinct. One possible explanation for this observation is that the HAZUS99 fragility curves were estimated based on analysis of one model building of this structural type, while the empirically-derived curves come from many buildings of the same structural type. Hence the performance of the particular building population of the same class is not uniform and for the close values of spectral displacement there are buildings in several damage states. Another source of difference between the HAZUS99 fragility curves and those developed in the project is that the empirical data tend to be concentrated at lower values of spectral displacement and in the lower damage states. For the curves representing higher levels of damage, only a small number of data points were used in the analysis, thus the parameters should be used with caution. Note also that the fragility curves in Figure 4a actually cross at a spectral acceleration value of about 0.9 inches, thus they should not be used beyond this level of displacement.

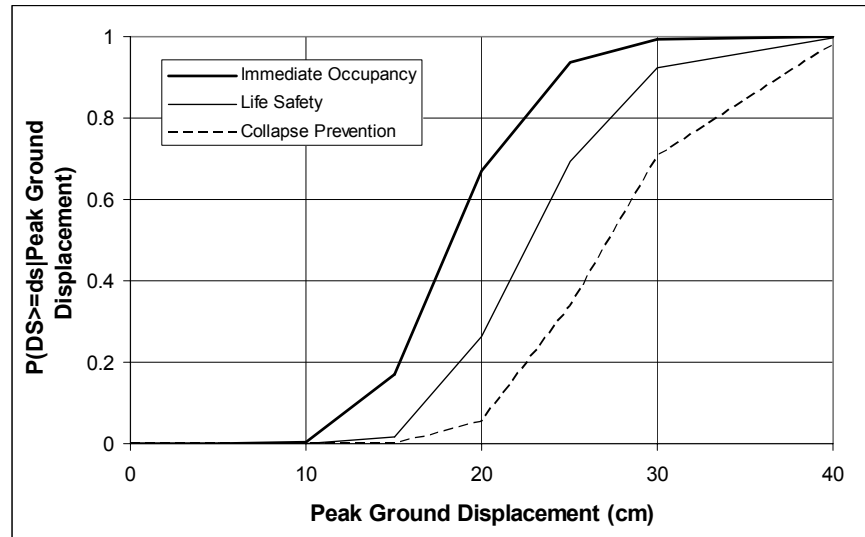
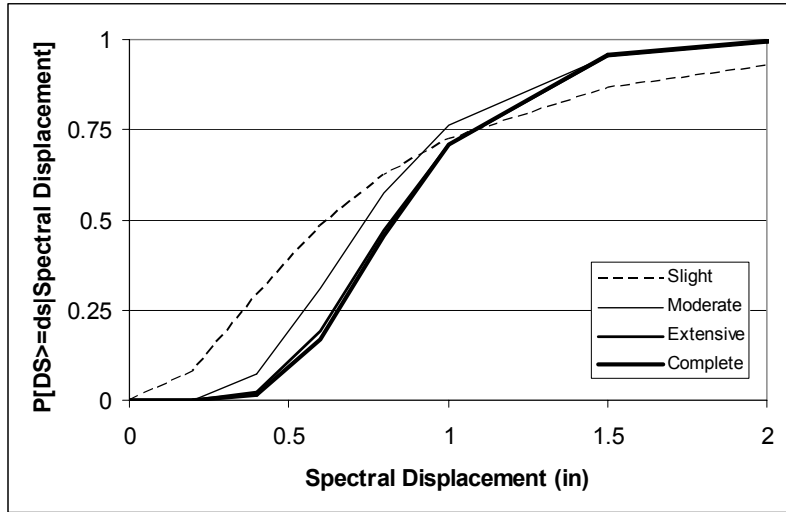


Figure 3 Lognormal fragility curves for W1 buildings and FEMA 273 performance levels, conditional on peak ground displacement.

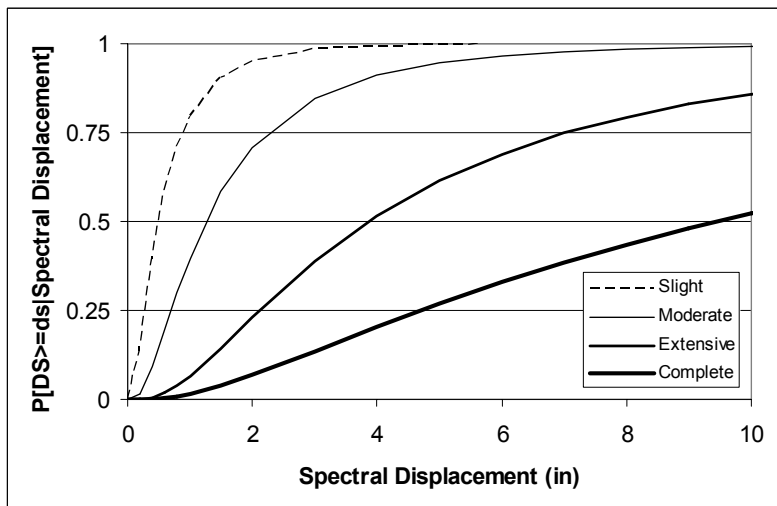
Damage probability matrices were developed for the same parameters for which the lognormal fragility curves were. The matrices were developed from the raw empirical data and also derived from the probability distributions defining the fragility curves. Those derived from the fragility curves are discussed here. The damage probability matrix in terms of Modified Mercalli Intensity (*MMI*) for the W1 building class can be compared to the DPMs published in ATC-13. Figure 5 shows the comparison of the DPM computed in the project for class W1 with the DPM published in ATC-13 for low rise wood frame buildings (class 1). As shown in Figure 5, the two damage probability matrices are quite different. The ATC-13 DPM, developed by fitting beta distributions to expert opinion data, shows a significant increase in probabilities of being in higher damage states for higher levels of *MMI*. Although, the empirically derived DPM (derived from the lognormal fragility curves) also shows an increase, it is very gradual. Most of the data points are at *MMI* levels of IX or lower, thus the probabilities associated with *MMI* X and XI should be used with caution. Note also that the ATC-13 DPM reflects a much narrower probability distribution on damage at each *MMI* level.

Relationships between building performance and strong ground motion are most commonly used for regional and site specific earthquake damage and loss estimation, with the resulting estimates providing information for purposes such as emergency response planning, probabilistic risk assessment, and performance-based design. A few of the relationships developed in this project are discussed above; however, based on this information alone, it is not possible to assess the quality and potential use of the motion-damage relationships. A more meaningful assessment is based on the results of the application of the relationships, i.e., the resulting regional and site-specific damage and loss estimates.

The HAZUS99 (FEMA, 1999) software was used to assess the motion-damage relationships developed in the project. The study region was Los Angeles County. The software was run using the ShakeMap (USGS, 2003) developed for the M 6.7 1994 Northridge



(a)



(b)

Figure 4 Fragility curves for W1 buildings, (a) computed in the project and (b) from HAZUS99.

earthquake; first with the default lognormal fragility parameters. Next, the fragility parameters developed in this project for the W1, W2, S1, C1, and C2 building classes were used to replace the default fragility parameters for the corresponding building classes in the HAZUS software. The replacement procedure followed that outlined in Porter et al. (2001). The results of the HAZUS analysis using the default and replaced fragility parameters with the 1994 Northridge earthquake ShakeMap are given in Table 3, which compares the number of buildings in each damage state by general structural class. In general, the number of buildings in the damage states of None and Complete increased significantly, while the number of buildings in the Slight, Moderate, and Extensive damage states decreased. The wood frame buildings show results that are similar to the total building inventory, as would be expected since they make up approximately 92% of the inventory. For concrete frame buildings, the number in the None and

Slight damage states changed very little, but there was a significant shift in the number of buildings from the Extensive and Complete damage states to the Moderate damage state. For the steel frame buildings, the number of buildings in the None damage state increased with the number in the other damage states decreased.

Damage State	Modified Mercalli Intensity					
	VI	VII	VIII	IX	X	XI
1-None	0.817	0.787	0.760	0.734	0.709	0.687
2-Slight	0.134	0.148	0.159	0.168	0.175	0.180
3-Light	0.030	0.037	0.043	0.048	0.053	0.057
4-Moderate	0.010	0.013	0.016	0.019	0.022	0.024
5-Heavy	0.004	0.006	0.008	0.009	0.011	0.013
6-Major	0.001	0.002	0.002	0.003	0.004	0.004
7-Destroyed	0.004	0.008	0.013	0.019	0.027	0.036

(a)

Damage State	Modified Mercalli Intensity					
	VI	VII	VIII	IX	X	XI
1-None	0.037	~ 0	~ 0	~ 0	~ 0	~ 0
2-Slight	0.685	0.268	0.016	~ 0	~ 0	~ 0
3-Light	0.278	0.732	0.949	0.624	0.115	0.018
4-Moderate	~ 0	~ 0	0.035	0.376	0.760	0.751
5-Heavy	~ 0	~ 0	~ 0	~ 0	0.125	0.231
6-Major	~ 0	~ 0	~ 0	~ 0	~ 0	~ 0
7-Destroyed	~ 0	~ 0	~ 0	~ 0	~ 0	~ 0

(b)

Figure 5 **Damage probability matrix for W1 building class, (a) computed in the project and (b) from ATC-13.**

HAZUS-generated structural, nonstructural, and total building losses are compared in Table 4 by general structural class. For the three building classes with modified fragility parameters, the losses decreased, by more than 10% for structural loss. This is consistent with the increase in the number of buildings in the None damage state. Nonstructural loss did not change because nonstructural fragility parameters were not considered in the project. The decrease in total loss was almost insignificant (from \$16.93B to \$16.52B, or 2.4%) due to the fact that the nonstructural loss (which remains constant) comprised more than 80% of the total building loss. In the HAZUS software, replacement values for nonstructural components are typically 70 to 80% of the total replacement value of the building.

Site-specific damage and loss estimation was also done illustrate the use of the developed fragility curves for other ground motion parameters and other damage or performance characterization. Motion-damage relationships, regardless of the method used to develop them, are typically intended to represent the average behavior, with uncertainty, of a group of buildings

of similar type that are subjected to the same ground motion. The user needs to be aware of the limitations in applying these relationships to a single building, where the uncertainty on the performance of an individual facility can be greater than the uncertainty on the performance of a group of similar facilities. Further discussion of uncertainties is beyond the scope of the project; thus results are presented as expected values.

Table 3 HAZUS99 Results: Number of Buildings in Each Damage State by General Structural Class for Los Angeles County and 1994 Northridge Earthquake ShakeMap Using (a) Default Fragility Parameters and (b) Using Fragility Parameters Developed in Project

(a)

General Structural Class	Number of Buildings by HAZUS99 Damage State					TOTAL
	None	Slight	Moderate	Extensive	Complete	
Concrete	12,763	2,987	2,048	613	105	18,516
Mobile Home	32,814	8,802	8,394	3,814	1,566	55,390
Precast	11,193	2,216	2,440	745	162	16,756
Reinforced Masonry	26,664	4,837	4,850	1,801	303	38,455
Steel	13,542	1,918	2,324	747	113	18,644
URM	3,309	1,181	1,059	409	209	6,167
Wood	1,216,291	410,652	153,587	16,945	4,946	1,802,421
TOTAL	1,316,576	432,593	174,702	25,074	7,404	1,956,349

(b)

General Structural Class	Number of Buildings by HAZUS99 Damage State (% Change from Results Using Default Fragility Parameters)					TOTAL ¹
	None	Slight	Moderate	Extensive	Complete	
Concrete	12,732 (-0.2)	2,922 (-2.2)	2,832 (38.3)	43 (-93.0)	11 (-89.5)	18,540 (0.1)
Mobile Home	32,814 (0.0)	8,802 (0.0)	8,394 (0.0)	3,814 (0.0)	1,566 (0.0)	55,390 (0.0)
Precast	11,193 (0.0)	2,216 (0.0)	2,440 (0.0)	745 (0.0)	162 (0.0)	16,756 (0.0)
Reinforced Masonry	26,664 (0.0)	4,837 (0.0)	4,850 (0.0)	1,801 (0.0)	303 (0.0)	38,455 (0.0)
Steel	15,166 (12.0)	1,195 (-37.7)	1,635 (-29.6)	552 (-26.1)	112 (-0.9)	18,660 (0.1)
URM	3,309 (0.0)	1,181 (0.0)	1,059 (0.0)	409 (0.0)	209 (0.0)	6,167 (0.0)
Wood	1,696,471 (39.5)	75,427 (-81.6)	12,269 (-92.0)	2,551 (-84.9)	16,904 (241.8)	1,803,622 (0.1)
TOTAL	1,798,349 (36.6)	96,580 (-77.7)	33,479 (-80.8)	9,915 (-60.5)	19,267 (160.2)	1,957,590 (0.1)

¹ Changes in total number of buildings are due to round-off error in HAZUS99 software

Table 4 HAZUS99 Results: Building Loss by General Structural Class for Los Angeles County and 1994 Northridge Earthquake ShakeMap (a) Using Default Fragility Parameters and (b) Using Fragility Parameters Developed in Project

(a)

General Structural Class	Loss (\$×1,000)		
	Structural	Nonstructural	Total Building
Concrete	321,441	1,185,176	1,506,617
Mobile Home	51,753	124,631	176,384
Precast	344,032	870,492	1,214,524
Reinforced Masonry	354,523	1,271,606	1,626,129
Steel	331,943	1,070,631	1,402,574
URM	152,077	456,155	608,232
Wood	1,419,668	8,974,569	10,394,237
TOTAL	2,975,437	13,953,260	16,928,697

(b)

General Structural Class	Loss (\$×1,000)		
	Structural	Nonstructural	Total Building
Concrete	141,978 (-55.8)	1,185,176 (0.0)	1,327,154 (-11.9)
Mobile Home	51,822 (0.0)	124,631 (0.0)	176,453 (0.0)
Precast	344,031 (0.0)	870,492 (0.0)	1,214,523 (0.0)
Reinforced Masonry	354,527 (0.0)	1,271,606 (0.0)	1,626,133 (0.0)
Steel	258,899 (-22.0)	1,070,631 (0.0)	1,329,530 (-5.2)
URM	152,227 (0.0)	456,155 (0.0)	608,382 (0.0)
Wood	1,265,557 (-10.9)	8,974,569 (0.0)	10,240,126 (-1.5)
TOTAL	2,569,041 (-13.7)	13,953,260 (0.0)	16,522,301 (-2.4)

The motion-damage relationships are used to estimate damage and loss to a hypothetical single-story wood frame dwelling (W1) located in southern California. The purpose here is to not only illustrate the use of the motion-damage relationships, but also to compare and assess the reasonableness of the damage and loss results obtained using the various parameters from a single ground motion record. The ground motion parameters are based on the probabilistic seismic hazard for the site, obtained from the USGS National Seismic Hazard Mapping Program website (USGS, 2003). The time-dependent and frequency-dependent ground motion parameters

were computed following the same procedure as for the recorded ground motion used in the project. These parameters are listed in Table 5 for two seismic hazard levels. Table 6 lists the expected damage, in terms of percent loss, for a W1 building for each characterization of performance (i.e., ATC-13, HAZUS99, FEMA 273, and Vision 2000) for each 10% in 50 year hazard ground motion parameter for which reasonable lognormal fragility curves could be developed.

Table 5 Ground Motion Parameters Computed from Site-Specific Acceleration Data

Parameter	10% in 50 year Value	2% in 50 year Value
Peak Ground Acceleration (g)	0.74	1.18
Peak Ground Velocity (cm/sec)	43.1	127.3
Peak Ground Displacement (cm)	10.3	59.2
Total Record Duration (sec)	64	64
90% Cumulative Duration (sec)	7.0	6.0
Bracketed Duration (sec)	12.8	13.2
Root Mean Acceleration for Total Duration (g)	0.06	0.11
Root Mean Acceleration for 90% Duration (g)	0.18	0.33
Root Mean Acceleration for Bracketed Duration (g)	0.14	0.24
Arias Intensity (cm/sec)	409.3	1140.7
Acceleration Spectrum Intensity (g)	0.50	0.84
Effective Peak Acceleration (g)	0.50	0.83
Effective Peak Velocity (cm/sec)	40.8	73.4
Response Spectrum or Housner Intensity (cm/sec)	227.6	405.7
Modified Mercalli Intensity ¹	IX	X
ShakeMap Instrumental Intensity	8.0	9.7
Roof Drift Ratio (%)	0.17	0.29
Maximum Interstory Drift Ratio (%)	0.21	0.35
Spectral Displacement at Predominant Period ² (cm)	0.63	1.05
Spectral Velocity at Predominant Period ² (cm/sec)	27.9	46.3
Spectral Acceleration at Predominant Period ² (g)	1.26	2.09

¹ Computed using formula from Trifunac and Brady (1975), with rounding to nearest integer

² Predominant period for one-story wood frame building estimated as 0.14 sec.

The results in Table 6 show that, for the most part, the expected damage using the ATC-13 damage state characterization is slightly higher than for the other characterizations. The expected damage is in the range of 2-3% for the ATC-13 damage state characterization, in the range of 1-2% for the HAZUS99 and Vision 2000 characterizations, and less than 1% for the FEMA 273 characterization. There are a few outliers, for example the expected damage conditional on peak ground acceleration and conditional on MMI, which need further evaluation. Results using the 2% in 50 year hazard ground motion data are not shown here due to space limitations. They show more dramatic variation among the expected damage values based on the different ground motion parameters as well as among the different building performance characterizations. As discussed in the final project report, a possible explanation for the variation is that the motion-damage relationships were developed using data that do not

adequately represent the high levels of ground motion that correspond to a 2% in 50 year hazard level.

Table 6 Expected Damage for Example Site Specific Analysis of Single-Story W1 Building for 10% in 50 Year Hazard Ground Motion

Parameter	Expected Damage in Percent Loss by Damage or Performance Characterization Type			
	ATC-13	HAZUS99	FEMA 273	Vision 2000
Peak Ground Acceleration (g)	9.5	8.6	0.6	81.4
Peak Ground Velocity (cm/sec)	2.8	1.0	0.5	1.1
Peak Ground Displacement (cm)	5.7	1.0	0.5	1.0
Bracketed Duration (sec)	NA	1.3	0.6	1.3
Root Mean Acceleration for Total Duration (g)	3.9	NA	0.8	1.2
Effective Peak Velocity (cm/sec)	2.0	NA	NA	NA
Response Spectrum or Housner Intensity (cm/sec)	NA	NA	1.2	1.8
Modified Mercalli Intensity	13.4	NA	NA	NA
ShakeMap Instrumental Intensity	2.4	1.0	0.5	NA
Roof Drift Ratio (%)	3.7	2.4	1.7	2.0
Maximum Interstory Drift Ratio (%)	2.4	1.0	0.5	1.0
Spectral Displacement at Predominant Period (cm)	3.2	1.6	0.8	1.6
Spectral Velocity at Predominant Period (cm/sec)	3.0	1.5	0.8	1.5
Spectral Acceleration at Predominant Period (g)	2.5	2.0	1.3	2.0

Note: NA means that probability distribution parameters did not reach convergence.

Conclusions

Motion-damage relationships in the form of lognormal fragility curves and corresponding damage probability matrices have been developed from observed building performance data and recorded ground motion within 1000 feet of the buildings. The relationships are for wood frame, steel frame, and concrete frame buildings, for damage characterized by ATC-13 and HAZUS99 damage states and FEMA 273 and Vision 2000 performance levels, and for several ground motion and building demand parameters. A comparison to the ATC-13 and HAZUS99 published damage models shows that the models developed in the project are quite different. The difference is due primarily to the characteristics of the data used in the model development – there is a bias towards lower levels of ground motion and lower levels of damage. Despite the differences in the models themselves, when applied to regional loss estimation via the HAZUS99 software, the total losses for the study region are similar to those computed with the default fragility curve data. For site specific application, the results show that similar losses are produced using different ground motion parameters, and that damage or performance characterization has an influence on the loss values.

The project discussed in this paper utilized a systematic and rigorous method for developing motion-damage relationships from databases of observed building performance and nearby recorded strong ground motion. Although several relationships were developed in the project, the number of building types for which relationships could be developed was limited due to the lack of useful building performance datasets for several types of buildings. In addition, the range of strong ground motion and building demand parameters over which the relationships should be used is limited due to the lack of datasets corresponding to high levels of ground motion. It is hoped that these problems will be remedied by accurate and complete collection of performance data following future seismic events. Utilizing the methods outlined in this project, the developed motion-damage relationships can be updated when new data becomes available, and additional relationships can be developed for other model building types.

Acknowledgements

The authors would like to sincerely thank the following individuals who provided valuable data for use in the project: David Bonowitz, Bret Lizundia, and Chris Poland. Ayse Hortacsu provided help with the application of the fragility curves in HAZUS99.

References

- Anagnos, T., Rojahn, C., and Kiremidjian, A., 1995, *NCEER-ATC Joint Study on Fragility of Buildings*, Technical Report NCEER-95-0003, National Center for Earthquake Engineering Research, State University of New York at Buffalo.
- ATC, 2000, *Database on the Performance of Structures Near Strong-Motion Recordings: 1994 Northridge, California, Earthquake*, ATC-38 Report, Applied Technology Council, Redwood City, CA.
- ATC, 1985, *Earthquake Damage Evaluation Data for California*, ATC-13 Report, Applied Technology Council, Redwood City, CA.
- ATC, 1978, *Tentative Provisions for the Development of Seismic Regulations for Buildings*, ATC-3-06 Report, Applied Technology Council, Redwood City, CA.
- Camelo, V.S., Beck, J.L., and Hall, J.F., 2001, *Dynamic Characteristics of Woodframe Buildings*, CUREE-Caltech Woodframe Project Report, Consortium of Universities for Research in Earthquake Engineering, Richmond, CA.
- Chopra, A.K., Goel, R.K., and De la Llera, J.C., 1998, "Seismic Code Improvements Based on Recorded Motions of Buildings During Earthquakes," in *Proceedings of SMIP 98 Seminar on Utilization of Strong-Motion Data*, California Strong Motion Instrumentation Program, Division of Mines and Geology, Sacramento, CA.
- FEMA, 2000, *Recommended Seismic Evaluation and Upgrade Criteria for Existing Welded Steel Moment-Frame Buildings*, Report FEMA-351, Prepared by the SAC Joint Venture for the Federal Emergency Management Agency, Washington, DC.2000.
- FEMA, 1999, *HAZUS Earthquake Loss Estimation Methodology*, Technical Manual, Prepared by the National Institute of Building Sciences for the Federal Emergency Management Agency, Washington, DC.

- FEMA, 1998, *Handbook for the Seismic Evaluation of Buildings – A Prestandard*, Report FEMA 310, Prepared by the American Society of Civil Engineers for the Federal Emergency Management Agency, Washington, DC.
- FEMA, 1997, *NEHRP Guidelines for the Seismic Rehabilitation of Buildings*, Federal Emergency Management Agency, Report FEMA-273, Washington, DC.
- Heintz, J.A. and Poland, C.D., 2001, “Correlating Measured Ground Motion with Observed Damage,” *Earthquake Spectra*, Supplement A to Volume 17, pp. 110-130.
- Housner, G.W., 1959, “Behavior of Structures During Earthquakes,” *Journal of the Engineering Mechanics Division*, American Society of Civil Engineers, Vol. 85, No. EM14, pp 109-129.
- ICBO, 1997, *Uniform Building Code*, International Conference of Building Officials, Whittier, CA.
- King, S.A., Kiremidjian, A.S., Sarabandi, P., and Skokan, M., 2002, “Correlation of Observed Building Performance with Measured Ground Motion,” *Proceedings of the SMIP02 Seminar*, California Strong Motion Instrumentation Program, California Geological Survey, Sacramento, CA.
- Lizundia, B. and Holmes, W.T., 1997, “The performance of rehabilitated URM buildings in the Northridge earthquake,” *Proceedings of the NEHRP Conference and Workshop on Research on the Northridge, California Earthquake of January 17, 1994*, California Universities for Research in Earthquake Engineering (CUREE), Richmond, California, Vol. III-A, 1998, pages III-116 -- III-123.
- Miranda, E. and Reyes, C.J., July 2002, “Approximate Lateral Demands in Multistory Buildings with Nonuniform Stiffness,” *Journal of Structural Engineering*, Vol. 128, No. 7, pp 840-849.
- Miranda, E., April 1999, “Approximate Seismic Lateral Deformation Demands in Multistory Buildings,” *Journal of Structural Engineering*, Vol. 125, No. 4, pp 417-425.
- Porter, K.A., Beck, J.L., Seligson, H.A., Scawthorn, C.R., Tobin, L.T., Young, R., and Boyd, T., 2001, *Improving Loss Estimation for Wood Frame Buildings*, Final Report on Tasks 4.1 and 4.5 of the CUREE-Caltech Woodframe Project, CUREE, Richmond, CA.
- SEAOC, 1995, *Performance based seismic engineering of buildings (Vision 2000)*, Structural Engineers Association of California, Sacramento, CA.
- Singhal, A. and Kiremidjian, A.S., 1996, *A Method for Earthquake Motion-Damage Relationships with Application to Reinforced Concrete Frames*, John A. Blume Earthquake Engineering Center Technical Report No. 119, Stanford University, Stanford, CA.
- Trifunac, M.D and Brady, A.G., 1975, “On the correlation of seismic intensity with peaks of recorded strong ground motion,” *Bulletin of the Seismological Society of America*, Vol. 65, No. 1, pp 139-162.
- USGS, 2003, ShakeMap website, www.shakemap.org.
- USGS, 2003, National Seismic Hazard Mapping Project website, geohazards.cr.usgs.gov/eq/index.html

Wald, D.J., Quitariano, V., Heaton, T.H., and Kanamori, H., 1999, "Relationships between Peak Ground Acceleration, Peak Ground Velocity, and Modified Mercalli Intensity in California," *Earthquake Spectra*, Vol. 15, No. 3, pp 557-564.